6

The shear properties of woven fabrics

6.1 General shearing behaviour of woven fabrics

6.1.1 Introduction

Textile fabrics in practical use are subjected to a wide range of complex deformations. The shear properties of woven fabrics are of importance in many applications. To understand the mechanisms of fabric shear behaviour, Dreby (1941), Go *et al*. (1957), Morner and Eeg-Oloffson (1957), Kawabata (1972, 1980) and Kawabata *et al.* (1972) introduced their shear apparatus to measure fabric shear properties. Later, Cusick (1961), Lindberg *et al*. (1961) and Grosberg and Park (1966) found a qualitative means of describing shear properties using a model. They indicated that the hysteresis produced during shearing is determined wholly by the frictional restraints arising during rotation of the yarn from the intersecting points in the fabric. In addition, the existing literature proved that shear mechanism is one of the important properties influencing the draping, pliability and handle qualities of woven fabrics (Kawabata, 1980; Oloffson, 1967; Lloyd *et al*., 1978). Shear deformation of woven fabrics also affects the bending and tensile properties of woven fabrics in various directions rather than in the warp and weft directions only (Chapman, 1980; Skelton, 1976).

6.1.2 Shear stress–strain curve

Shear behaviour of woven fabrics has received wide attention. Up to now general stress–strain curve in shear has been considered as showing the characteristics that are illustrated in Fig. 6.1. If a fabric is deformed at low levels of strain, the OA region, the shear stiffness is initially large, and decreases with increasing strain. In this region, the shear behaviour is dominated by frictional mechanisms and the decreasing incremental stiffness is generally attributed to the sequential movement of frictional elements. As soon as the stress is large enough to overcome the smallest of the frictional restraints

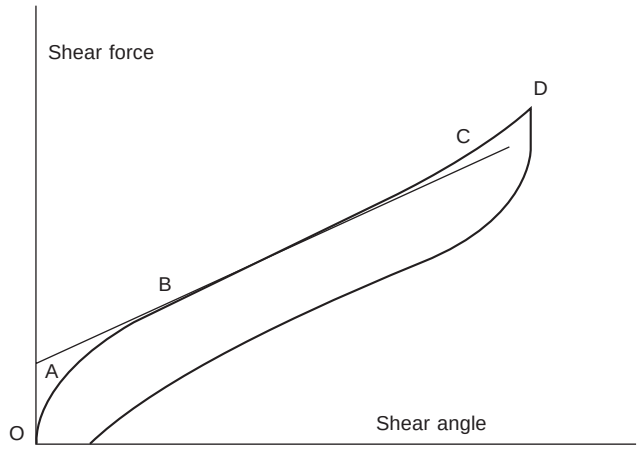

6.1 Stress–strain curve of woven fabrics during shear deformation.

that are acting at the intersection regions, the system starts to slip, and the incremental stiffness falls – this is the AB region. At a particular amplitude of stress, the incremental stiffness reaches a minimum level, point B, and remains almost linear over a range of amplitudes with slopes that are thought to be controlled by the deformation of the so-called 'elastic elements' in the fabric. It is a commonly observed fact that above a relatively low level of shear strain (5–10°), the shear stiffness increases with increasing strain. At amplitudes greater than a certain amount, point C, the incremental stiffness again begins to rise, and the closed curves increase in width with increasing amplitudes of shear angle. It seems that this is due to steric hindrance between the two bent intersectioning yarns, leading to transverse distortion of the yarns, or riding up of the intersection, or both.

There are two parameters used in most of the literature (three in the KES system) which control the extent of the non-linear region and characterise the general nature of fabric shear. These are the slope of the stress–strain curve where it attains its minimum value, and the hysteresis. The minimum slope of the curve represents the contribution of the so-called 'purely elastic elements' of the assembly and, when this value is achieved, it is assumed that all the frictional contact points are in motion. The decreasing stiffness region of the curve is of interest since it is here that the hysteresis loss in the cyclic deformation is determined.

6.1.3 Relationship between shear and bending deformations

Some authors have reported that the shear and bending of woven fabrics have a strong relationship. For example, it has been suggested that the shear

energy loss is a good guide to the kind of behaviour that can be expected in bending. Skelton thought that the shear and bending are not merely related but essentially identical (Skelton, 1980).

In a paper by Dawes and Owen (1971), the correlation between the two measurements of shear stiffness and bending stiffness is found to be quite good and the overall changes in mechanical properties as the environmental conditions change are very similar in the two modes of deformation. Thus it was believed that they share a common origin.

Skelton further argued that, for instance, for a shear angle of a few degrees (5°), and a fabric with 20 threads/cm, the effective curvature in the yarn is:

$$\frac{5 \times 20}{57} \approx 2 \text{ cm}^{-1} \qquad [6.1]$$

This is typical of the curvature levels that have been investigated in studies of fabric bending behaviour. Thus the magnitude and distribution of the curvature in the yarns in the bent state are almost identical to those in the sheared state.

6.2 Modelling of shearing behaviour of woven fabrics

6.2.1 Theory

Several authors have attempted a structural analysis to predict shear properties, but the conclusions reached differ in some respects and in addition the calculations are not presented in a form that can be readily put to practical use (Mark and Taylor, 1956; Morner and Eeg-Olofsson, 1957; Lo, 2001; Lo and Hu, 2002; Behre, 1961; Cusick, 1961; Postle *et al.*, 1976; Skelton, 1976). It is recognised that the detailed mechanisms which are operating are extremely complex and it is difficult to devise a convincing model that is adequate to explain them. However, the shear behaviour, especially in the initial region, is thought by some authors to be controlled by elastic and frictional elements simultaneously. In a general sense the behaviour of an array of elastic and frictional components has been studied by Oloffson (1967), and by Skelton (1976) and Skelton and Schoppee (1976). As discussed in the previous chapter, some of the existing literature put forward the belief that the stress–strain behaviour of a series of assemblies similar to frictional–elastic units can be reasonably represented in the initial, non-linear region of shear by an expression of the form:

$$\sigma = K\varepsilon^{1/2} \qquad [6.2]$$

where σ and ε are the shear stress and strain respectively and k is the material constant. This is the simplified Oloffson formula which is the same as the bending deformation.

6.2.2 Relationship between shear stiffness and hysteresis of woven fabrics

Figure 6.2 gives an example of the tested relationships between shear stiffness G and shear hysteresis $2HG$ and $2HG5$. It can be seen that, as in bending deformation, their relations are linear. The correlation coefficients can be as high as 0.9507 for G and $2HG$, and 0.9683 for G and $2HG5$. This may indicate, as discussed in Chapter 5 on bending properties, that friction exists during the whole shear process and not only in the initial region, because the hysteresis is mainly caused by the frictional element, especially $2HG$. In addition, friction and elastic elements always exist simultaneously. Thus it

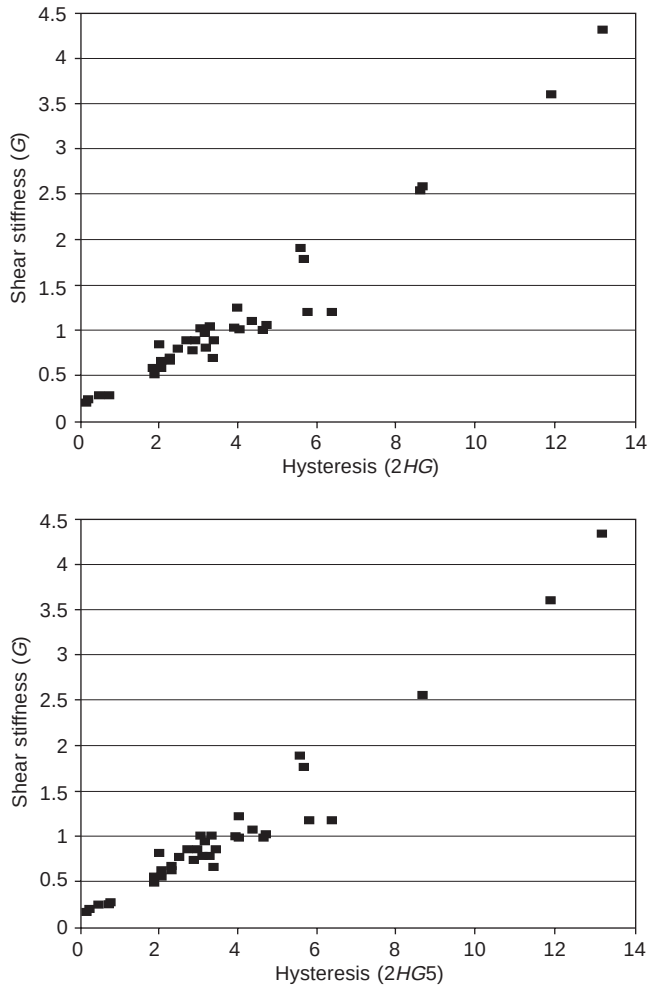

6.2 Shear stiffness vs shear hysteresis.

may not be appropriate to say that there is a pure elastic region, but the frictional effect is continuous throughout the entire shear process. The decreased value of shear stiffness after the initial region is attributable to the value of the dynamic friction coefficient being smaller than that of the static friction one.

6.2.3 Fitting of shear curves using non-linear regression

Since the friction and elastic elements exist simultaneously in the whole shear process before the steric hindrance occurs or in the earlier stage of shear, the stress–strain curves are assumed to be controlled by the combination of friction and elastic elements. As we saw Chapter 5, the application of the Oloffson model, in which the friction and elastic elements are considered simultaneously, is quite successful. In addition, in shear as in bending, it is also observed that shear stiffness and shear hysteresis are very closely related. This leads to the present attempt to extend the stress–strain relationship described in equation 6.2 to the following for shear deformation before steric hindrance occurs:

$$\sigma = \alpha \varepsilon^{\beta} \qquad [6.3]$$

where α and β are non-linear regression constants. The non-linear regression method is again used for estimating the constants in the equation.

Some of the shear stress–strain curves tested on the KES system, which are thought to be within the friction and elastic operating region or not involved in steric hindrance, are chosen for fitting the model; their fitted curves are given in Fig. 6.3, which shows that the tested and the calculated data are in reasonably good agreement with each other. A typical plot of tested stress and calculated stress is shown in Fig. 6.4, which indicates clearly a straight line between them.

The correlation coefficients are close to 1; but it should be noted that residuals from them are still larger than those we observed in the modelling of bending curves. Equation 6.3 is good enough to model the initial part of the shear curve of woven fabrics. In addition, shear angle also plays a part in the modelling effect of equation 6.3. For example, equation 6.3 is better used to model a KES shear curve with a maximum shear angle of 1° than 8°.

However, in practice, in many cases, this initial region is so short that it may be unnecessary to give an exact mathematical description. Thus, from the above, the modelling of shear curves using equation 6.3 cannot be described as a success. As a result, different methods for modelling a shear curve should be adopted to meet different needs. For example, if an analysis is confined to the small strain range, say, < 8°, i.e. the tested shear curve of a fabric within this is generally in the initial non-linear region or the maximum stress is smaller than or close to the minimum stiffness point, it can be

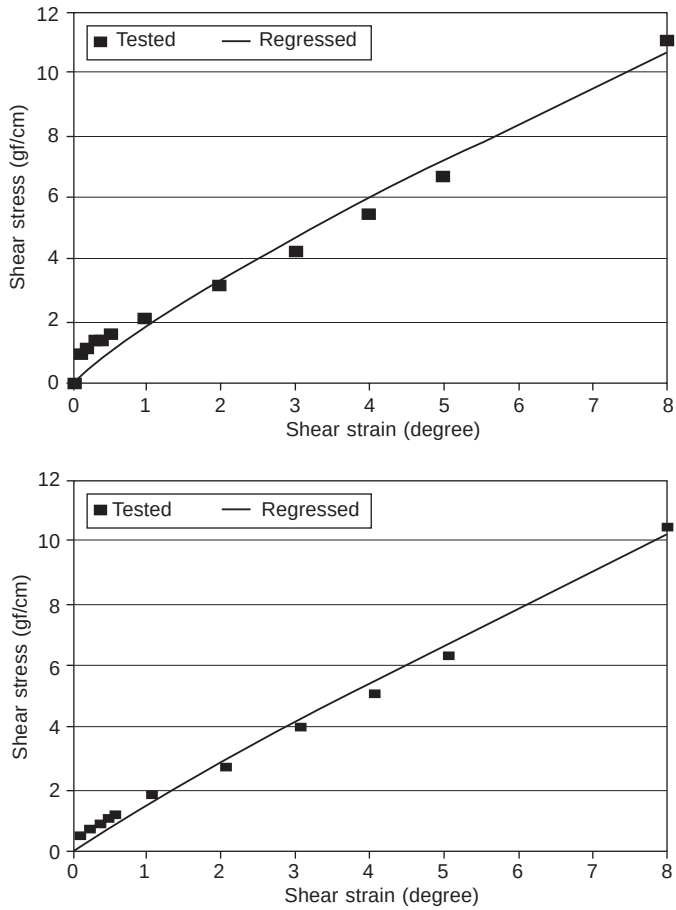

6.3 Tested and regressed shear curves.

modelled using equation 6.3; if the shear stress–strain curve is much beyond this minimum stiffness point, the curve cannot be modelled in this way, but a numerical method such as cubic-spline-interpolation may be more applicable; if the curve has a long close-to-linear range and the initial non-linear range is difficult to define or the maximum shear angle for minimum stiffness point is close to 0, it may be convenient to use the constant G provided by the KES system in which a straight line can be found.

6.2.4 Shear stiffness

In view of the complexity of the observed shear behaviour it is perhaps unreasonable to speak of shear stiffness as a single entity. We are concerned rather with the overall stress–strain characteristic of the fabric, and with an

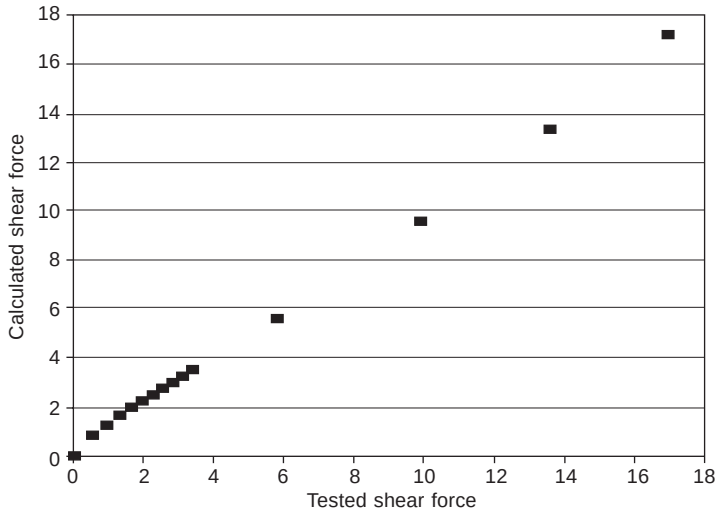

6.4 Tested and calculated shear stress.

understanding of the mechanisms operating when a fabric undergoes shear deformation. However, for a fabric like sample 18, if the shear condition is limited within 8° strain, the stress–strain curve may be modelled using the power function proposed by Oloffson, equation 6.3. Thus the shear stiffness may be found by differentiating the stress–strain function with respect to strain as shown in Fig. 6.5. It should be noted that the stiffness calculated is usually larger than that of the tested *G*. Therefore if the application needs high accuracy and continuous shear stiffness, it may be reasonable to use other numerical methods such as cubic-spline-interpolation to model it. In

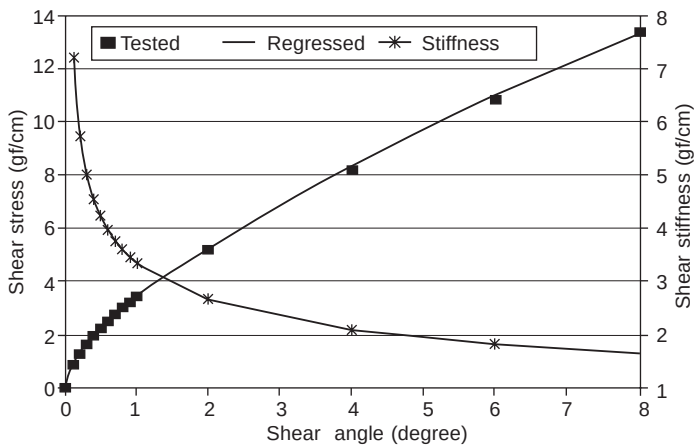

6.5 Comparison of fitted curves and KES tested data.

some cases, if a continuous stiffness is not strictly required, it may be convenient to use the KES constant shear stiffness *G*.

Generally speaking, the initial part of the shear curve can be modelled with a power function like equation 6.3. If continuous shear stiffness is required in some cases in the initial region, the equation is still accurate enough to be used for finding shear stiffness.

6.2.5 Comparison of warp and weft direction properties

The warp values of the shear properties, *G*, 2*HG* and 2*HG*5, can be compared with those in the weft. The results indicate that the values of the warp and weft 2*HG* and 2*HG*5 have no obvious differences if the warp and weft direction have similar yarns and similar cover factors, but *G* has marginally larger warp values. At the same time, the results also show that the larger the cover factor the larger the values of *G*, 2*HG* and 2*HG*5. Unlike the situation in bending, the hardening in the warp direction of woven fabrics seems to have little effect on the shear properties. This contradicts the argument that shear behaviour is identical in nature to bending properties. Perhaps a reasonable explanation may be jamming in the warp direction for high-density fabrics. That is, the larger values of *G*, 2*HG* and 2*HG*5 in the warp direction for the high-cover-factor fabrics are caused by the jamming effect. However, this jamming effect is not so prominent in fabrics with low-cover-factor or similar cover factors in the two principal directions. This suggests that the jamming effect may happen at a much earlier stage than the usually stated shear angle of 5–8°. The friction in shear exists mainly at the interface of the two systems of yarns, but inter-fibre friction within a yarn occurs in bending. This can be seen from the relationship between shear properties and cover factor.

6.2.6 Relationship between cover factor and shear properties

Figure 6.6 shows the general relationship between cover factor and the shear parameters *G*, 2*HG* and 2*HG*5, which is obtained from Fig. 6.7. According to this figure, we may find that when the ratio of warp and weft cover factor is smaller than 1.4, the increase in the ratio of cover factor causes an increase in the ratio of shear hysteresis 2*HG*; when the ratio of cover factor is greater than 1.5, the ratio of 2*HG* is almost certain to remain constant. This is because when the actual cover factor is larger than 100 %, further increase of the cover factor in most cases does not increase the actual contact area between the two systems of yarns. Another factor is that the relation of *G* and 2*HG* to the cover factor is similar to that of 2*HG*.

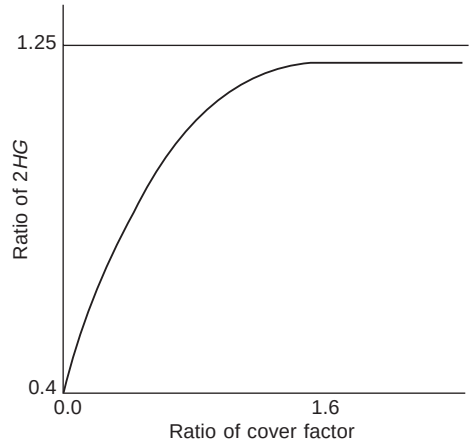

6.6 Generalised relationship of shear property and cover factor.

6.2.7 Relationship between bending and shear behaviour

Figure 6.8 illustrates the plots of bending properties against shear properties for cotton fabrics. It is clear that the dots have some trends, but these trends seem rather obscure. All this may indicate that they do have some relationship in some cases but not in all.

The comparison of warp and weft direction properties in Chapter 4 reveals that strain-hardening in the warp direction in woven fabrics hardens the bending behaviour as well; but it seems to have little significance for shear behaviour because there are no trends showing that the warp values of G, $2HG$ and $2HG5$ are larger than those of the weft when the cover factors and the yarn properties are similar. This suggests that the mechanisms operating in bending and shear may be different.

The results analysed above suggest that bending and shear may have some relationship, but that this relationship is not always as strong as described in some of the existing literature and that, in some cases, they are different in nature. Mechanically speaking, the two deformation modes both involve the friction and bending of yarns, but these two mechanisms are operating in different ways, especially the frictional effect. The inter-fibre friction in shear seems to be less important than it is in bending; thus the hardening of warp yarns of woven fabrics, which affects the internal friction, has little effect on shear behaviour.

6.3 Testing of shear properties

6.3.1 Introduction

The appearance of garments on human bodies has always been the prime concern of both fabric and garment designers. Up to now, design of fabric

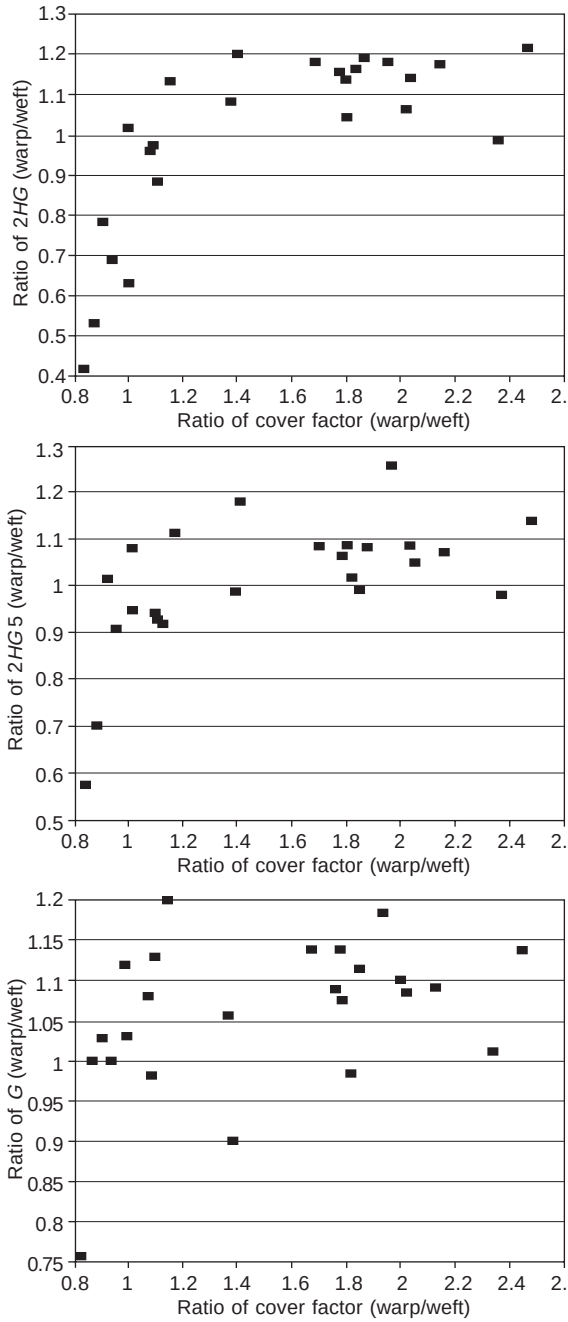

6.7 Relationship between cover factor and shear parameters.

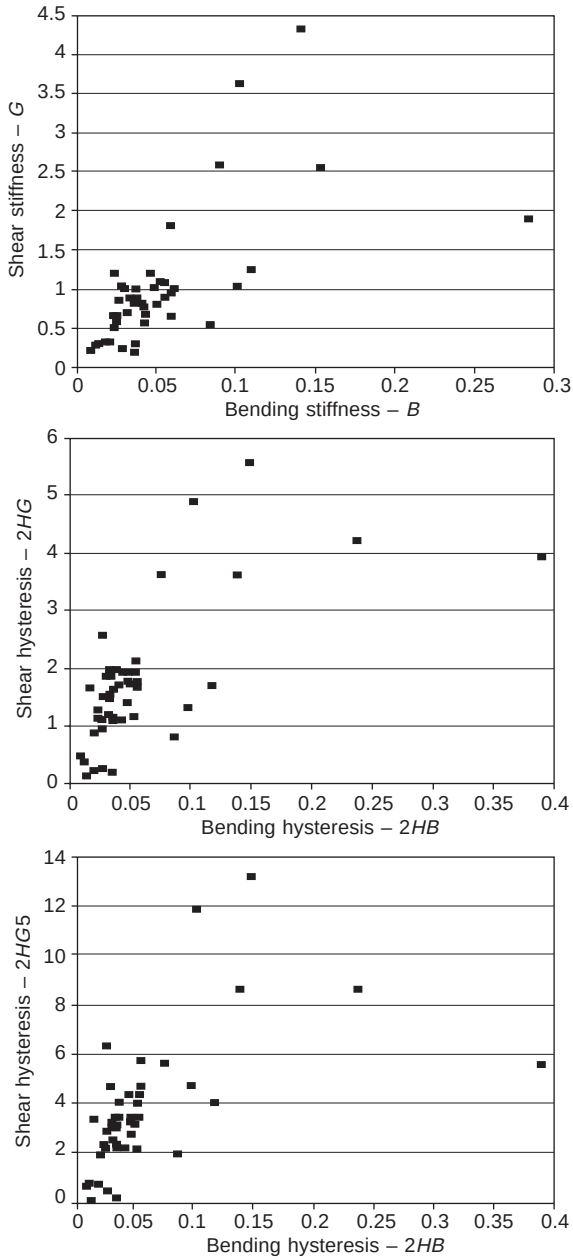

6.8 Relationship between shear and bending properties.

and garments has relied heavily on past experience and trial-and-error. As textiles and clothing products, dictated by modern fashion trends, move through ever faster cycles of renewal, just-in-time and quick response are becoming ever more important in the textiles and clothing industries. Consequently, modern technologies such as computer-aided design (CAD) are attracting increasing attention. The development of advanced CAD systems capable of simulating complex fabric deformations on human bodies will have great benefits for the textiles and clothing industries: faster industry responses to market demands, higher product quality, more variety, and reduced production costs.

While there have been a significant number of attempts to develop clothing CAD systems (Okabe and Akami, 1984; Collier *et al.*, 1991; Gan *et al.*, 1991; Kang *et al.*, 1994), progress has been hindered by the lack of ability to simulate the true appearance of fabrics on computers. No reliable and efficient technique currently exists for the numerical prediction of complex fabric deformations, which generally involve buckling and post-buckling large deformations, large rotations, material non-linearities, and complex interactions between the fabric and the human body. In this section, an attempt will be reported to establish an appropriate non-linear constitutive model for fabric materials in the analysis of fabric complex deformations, an area in which several difficulties currently exist.

Fabrics are generally treated as orthotropic thin sheets in a numerical model (e.g. finite-element shell model). The tensile membrane and bending properties determined by existing test procedures, e.g. the KES system (Kawabata, 1980), are suitable for direct use in constitutive models, but there are difficulties in translating the shear modulus obtained from the KES shear tester into a sensible figure for the true shear modulus.

Because fabrics are susceptible to buckling under external forces, it is very difficult to design perfect shear test equipment. The KES shear tester is the only commercialised one for fabrics so far, and it is widely used for various applications, such as fabric hand and tailorability evaluation. This existing test procedure for fabric shear modulus involves a piece of rectangular cloth clamped along two opposite edges and free on the other two edges. During the test, the cloth is pre-tensioned and then subjected to shear forces on the clamped edges which undergo relative displacements as a result of the applied shear forces as shown in Fig. 6.9. The deformations and forces in the cloth so loaded do not correspond to a pure shear state as achieved in a conventional shear test for other engineering materials in Fig. 6.10. Therefore, the test result cannot lead directly to the determination of the fabric shear modulus, particularly in the non-linear range of stress–strain relationship.

It is desirable to obtain an analytical solution for the problems advanced above. In applied mechanics, there exists an analytical solution to the shear stress or strain distribution on the specimen used, as shown in Fig. 6.9 for

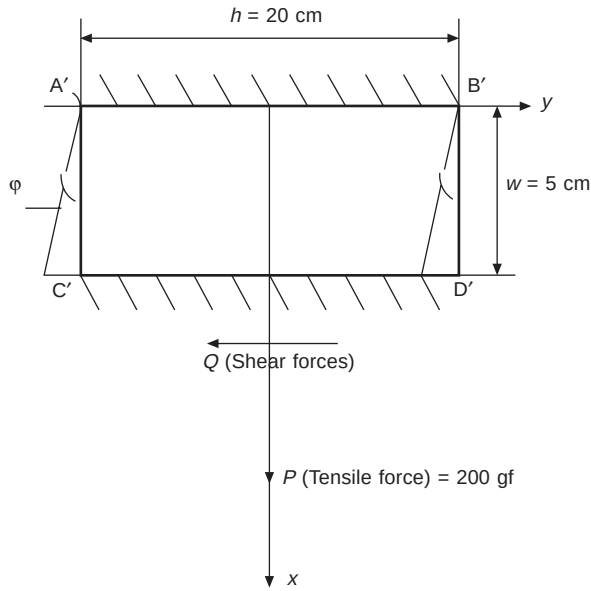

6.9 The KES shear testing apparatus.

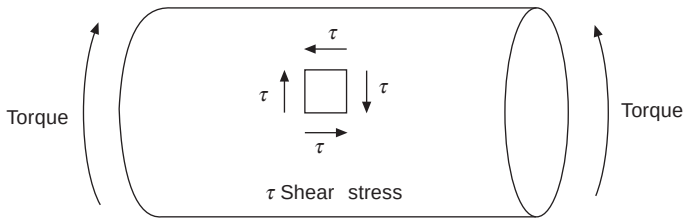

6.10 Conventional test to determine the shear modulus of a stiff material.

homogenous isotropic materials. However, no existing analytical solution for orthotropic materials can be found in the literature. Textile fabrics are not homogeneous isotropic materials, and no analytical solution has been presented for the fabric specimen in the KES shear tester.

6.3.2 The KES shear test

A schematic diagram for a specimen under KES shear test has been shown in Fig. 6.9. The size of the fabric specimen is 20 cm × 20 cm and the tested area is 20 cm × 5 cm. On this specimen, a tension of 10 gf/cm is imposed along the clamped sides of the fabric in the *x* direction to avoid buckling of the fabric. During the test, the cloth is subjected to shear forces on the clamped edges which undergo relative displacements along the *y* axis as a

result of the applied shear forces. The angle φ represents the rotation of a point on the moving edge of the tested specimen, but not the shearing strain. The maximum angle of rotation in this test is 8° which corresponds to the wearing condition of fabrics. It is possible to find the forces exerted on the specimen, although the general loading condition and shear stress distribution of the specimen are complicated.

According to the equilibrium conditions in the *X–Y* plane in Fig. 6.9, the following equations can be obtained:

$$\sum X_i = 0 \qquad [6.4]$$

$$\sum Y_i = 0 \qquad [6.5]$$

and

$$\sum M_i = 0 \qquad [6.6]$$

where X_i represents a force in the *x* direction, Y_i a force in the *y* direction and M_i a moment in the *X–Y* plane. From these relations, it is clear that the specimen is subject to a tensile force of *P*, a pair of shear forces *Q* and moments $M_1 = M_2 = Q_w$. The forces and moments exerted on the specimen in the KES shear tester are shown in Fig. 6.11.

From the above loading condition, shear stress distribution on the specimen is not uniform. It is obvious that the shear stresses at the points on the left and right edges of the specimen are always zero in the whole loading process. Thus infinitesimal element B in Fig. 6.11 has only tensile stress, but element *A* has shear stress τ, and tensile stress σ.

The conventional test to determine shear modulus for stiff engineering materials is shown in Fig. 6.10, in which a circular rod is subject to torsional deformations. Thus, the element in the circular rod is subjected to pure shear deformation. By contrast, the KES shear tester does not produce a pure shear state in the tested specimen.

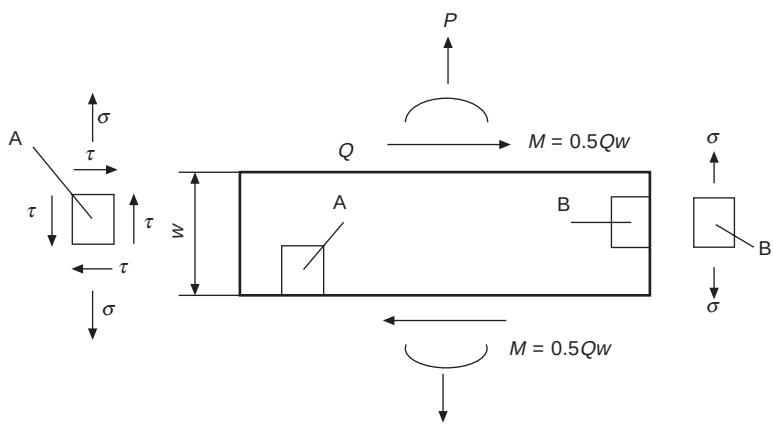

6.11 Forces exerted on fabric specimen under KES shear test.

There are two ways in which fabric mechanics researchers obtain shear modulus. One is the average slope of the shear curve when the shear angle is from 0.5–5° and the shear stress–strain relationship is simplified as linear. The other method is to find the derivative of the stress–strain curve when the shear stress–strain relation is considered as non-linear. Because the data obtained from the KES test does not correspond to pure shear, the force–rotation relationship and shear modulus derived are not applicable for numerical computation in the analysis of fabric complex deformations.

6.3.3 Finite-element analysis

From Fig. 6.11, it is clear that the shear stress distribution on the tested specimen is not uniform. In order to find out the general pattern of the shear stress (therefore strain) distribution, a finite-element analysis has been applied. To examine the typical distribution of shear stress in a KES test specimen, a finite-element analysis using 8-nodal plane-stress elements of the LUSAS finite-element package was carried out (Lucas, 1994). A linear elastic orthotropic material sheet was assumed and the constitutive law of orthotropic materials is:

$$\begin{Bmatrix} \sigma_x \\ \sigma_y \\ \tau_{xy} \end{Bmatrix} = \begin{bmatrix} c_{11} & c_{12} & 0 \\ c_{12} & c_{22} & 0 \\ 0 & 0 & c_{33} \end{bmatrix} \begin{Bmatrix} \varepsilon_x \\ \varepsilon_y \\ \gamma_{xy} \end{Bmatrix} \qquad [6.7]$$

where γ is shear strain, c_{11} and c_{22} are related to the tensile moduli E_1 and E_2 in the x and y directions respectively, c_{33} is the shear modulus and c_{12} is related to the Poisson's ratio. In finite element analysis, the material properties used are E_1 = 0.1096 MPa, E_2 = 0.0505 MPa, shear modulus C_{33} = 0.38 and Poisson's ratio ν = 0.1. The shear force applied on the specimen is 0.1 N/mm, which correspond to the properties of an ordinary fabric and loading condition in the KES shear test. The deformed shape of the specimen is shown in Fig. 6.12. In this figure, the coarsely meshed area simulates the clamping of the jaw of the KES shear tester in the longer direction, while the finer mesh area simulates the fabric specimen. The stress distribution in the x and y directions are shown in Figs 6.13 and 6.14. It can be seen from these figures that the stress is close to constant along the shorter direction while assuming a symmetrical curve in the longer direction.

6.3.4 Theory

6.3.4.1 Shear deformation of the specimen

The above finite-element analysis provides the general picture for the stress distribution in the specimen. It is desirable to obtain an analytical solution

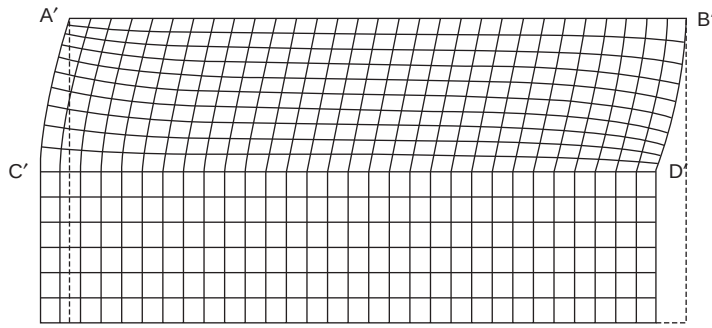

6.12 Deformed fabric specimen calculated by finite-element analysis.

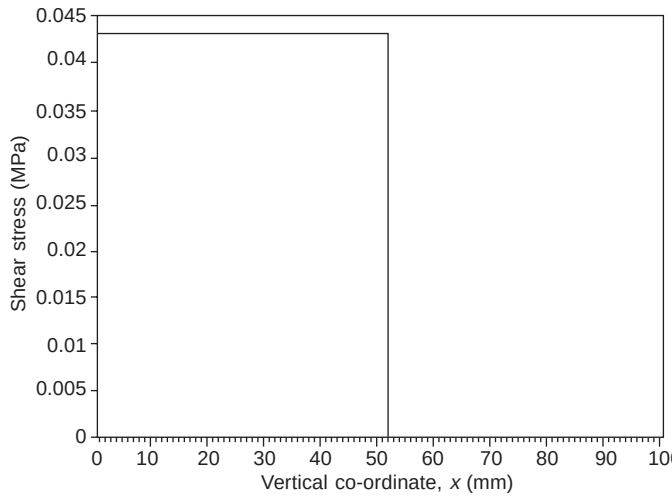

6.13 Shear stress variation along the shorter direction of the specimen.

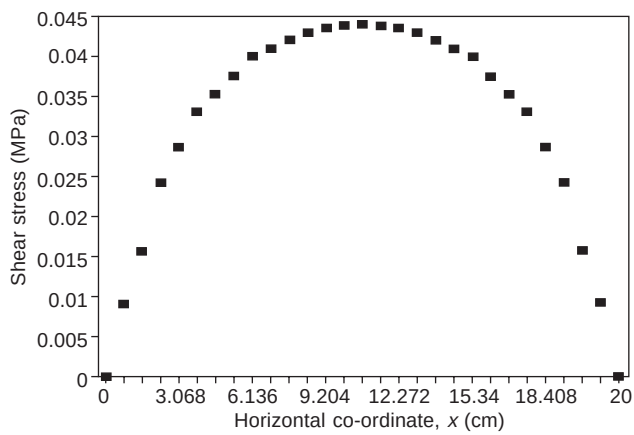

6.14 Shear stress variation along the longer direction of the specimen.

for the problem so that the exact relationship between test data and those for pure shear deformation can be obtained. The present study started with the application of the virtual work principle.

Fabric shear stress–strain relationship is usually non-linear. In order to simplify the equations, fabric material is considered to be linear and orthotropic, within a small incremental loading range from Q_n to Q_{n+1}, or Q. In this way, the results are applicable for non-linear material in the whole deformation process, during which many incremental steps for loading are taken. According to the principle of virtual work, the governing equations for plane stresses must satisfy the condition:

$$\int\int_{v} \int(\sigma_x \delta\varepsilon_x + \sigma_y \delta\varepsilon_y + \tau_{xy}\delta\gamma_{xy})\mathrm{d}V - \int_{S_1} \int(F_{nx}\delta u + F_{ny}\delta v)\mathrm{d}s = 0 \qquad [6.8]$$

In this equation, σ_x, σ_y are the stresses in the x and y directions respectively, and τ_{xy} the shear stress. $\delta\varepsilon_x$, $\delta\varepsilon_y$ and $\delta\gamma_{xy}$ are virtual strains. δu and δv are the virtual displacements along the x and y directions. F_{nx}, and F_{ny} are external distributed forces on the force boundaries. The first integral in the equation is with respect to the whole volume, while the other one for the integration on the force boundaries, ds, is related to fabric width and length.

In the case of a non-linear material, all stresses represent the values within an infinitesimal range of $Q(Q_n, Q_{n+1})$, within which the stress–strain relationship can be considered as linear.

6.3.4.2 Shear strain distribution

In order to apply the above governing equations to obtain the stress distribution in the test specimen, it is necessary to set up the displacement field which should satisfy the displacement boundary conditions and agree with the results obtained from the finite-element analysis. u and v in the following two equations form the displacement field in the x and y directions:

$$u = u_0 + \sum_{i=1}^{n} a_i u_i \qquad [6.9]$$

and

$$v = v_0 + \sum_{i=1}^{n} b_i v_i \qquad [6.10]$$

where u_0 and v_0 are the displacements on the prescribed displacement boundary, and θ_i and b_i are the projection values in the x and y directions, respectively. In the present case, on boundary A′B′ in Fig. 6.9, u_0 and v_0 are zero because

the fabric edge is fixed during testing. In addition, because the two edges of the fabric are clamped, the partial derivatives of the displacements on A′B′ are also zero. Thus: $u_0 = v_0 = 0$. In order to facilitate the computation, the following series are selected for trial functions:

$$u = u_0 + a_1 u_1 \quad [6.11]$$

and

$$v = v_0 + b_1 v_1 \quad [6.12]$$

where

$$u_1 = x \quad [6.13]$$

and

$$v_1 = x\cos\left(\frac{\pi}{h}y\right) \quad [6.14]$$

Therefore, the corresponding strains in the x–y plane can be expressed as equations 6.15–6.17:

$$\varepsilon_x = \frac{\partial u}{\partial x} = a_1 \quad [6.15]$$

$$\varepsilon_y = \frac{\partial v}{\partial y} = -b_1 \frac{\pi}{h} x \sin\left(\frac{\pi}{h}y\right) \quad [6.16]$$

and

$$\gamma_{xy} = \frac{\partial u}{\partial y} + \frac{\partial v}{\partial x} = b_1 \cos\left(\frac{\pi}{h}y\right) \quad [6.17]$$

Shear strain distribution follows the pattern described in equation 6.17. That is, the shear strain along x axis is constant, in other words, there is no strain variation along the x axis, while a cosine relation of strain holds along the y axis.

6.3.4.3 Shear stress distribution

According to equation 6.7, plane stresses can be obtained as the following:

$$\sigma_x = c_{11}\varepsilon_x + c_{12}\varepsilon_y = c_{11}a_1 - c_{12}b_1 \frac{\pi}{h} x \sin\left(\frac{\pi}{h}y\right) \quad [6.18]$$

$$\sigma_y = c_{12}\varepsilon_x + c_{22}\varepsilon_y = c_{12}a_1 - c_{22}b_1 \frac{\pi}{h} x \sin\left(\frac{\pi}{h}y\right) \quad [6.19]$$

and

$$\tau_{xy} = c_{33}\gamma_{xy} = c_{33}b_1 \cos\left(\frac{\pi}{h}y\right) \quad [6.20]$$

From equation 6.20, the shear stress along the x axis is constant, or there is no stress variation along the x axis, while a cosine relation holds along the y axis. This agrees with the numerical results shown in Figs 6.13 and 6.14 from the above finite-element analysis.

6.3.4.4 *Constants in the equation*

The constants a_1 and b_1 in the above equations are unknown so far. They can be obtained from the following analysis. According to the virtual displacement principle represented in equation 6.8, the following equations can be obtained:

$$\int\int_V \int \left(\sigma_x \frac{\partial u_1}{\partial x} + \tau_{xy} \frac{\partial u_1}{\partial y} \right) \mathrm{d}V - \int_S \int F_{nx} u_1 \mathrm{d}s = 0 \qquad [6.21]$$

and

$$\int\int_V \int \left(\tau_{xy} \frac{\partial v_1}{\partial x} + \sigma_y \frac{\partial v_1}{\partial y} \right) \mathrm{d}V - \int_S \int F_{ny} v_1 \mathrm{d}s = 0 \qquad [6.22]$$

Substituting equations 6.13–6.20 into equations 6.21 and 6.22, we get

$$a_1 = \frac{\Delta P}{c_{11} h t} \qquad [6.23]$$

and

$$b_1 = -\frac{3\pi h \Delta Q}{2(3c_{33} t h^3 + c_{22} \pi^2 t w^2)} \qquad [6.24]$$

where h is the width of the specimen, t the thickness of the fabric. P is the amount of the increment of tensile force which corresponds to the pretension applied to the specimen. Q is the shear force increment from (Q_n, Q_{n+1}), and c_{11} and c_{22} can be tested from the KES tensile tester. However, c_{33}, the shear modulus cannot be determined directly from the KES shear tester, but needs to be modified.

6.3.4.5 *Shear modulus*

The following procedure is used to find c_{33}. The calculation of c_{33} needs the values of the displacement increment v of the specimen corresponding to the force increment Q. According to equations 6.12 and 6.14, the displacement of the specimen is not uniform along the y axis; it is necessary to find out the equivalent average displacement. This requires the unit force on the specimen edge. If the total force applied on the specimen edge is Q, it can be found that the distribution of unit force on the edge where $x = w$ is

$$\frac{\pi}{2h}\cos\left(\frac{\pi}{h}y\right) \qquad [6.25]$$

According to the equivalency principle, the equivalent displacement increment, v, of the points at $x = w$ should be determined by

$$1^{*}\ \Delta v = \int_{\frac{h}{2}}^{\frac{h}{2}} \frac{\pi}{2h}\cos\left(\frac{\pi}{h}y\right)\cdot b_1 w\cos\left(\frac{\pi}{h}y\right)\mathrm{d}y = \frac{\pi}{4}b_1 w \qquad [6.26]$$

According to equation 6.12, $b_1 w$ is the displacement in the middle point of the specimen where $y = 0$. Thus the equivalent v is $\pi/4$ times the displacement of the middle point along the moving edge of the specimen.

The value of v so obtained is usually smaller than the actual one, thus a factor is required to modify it. The average value is taken between the maximum and the minimum:

$$k = \frac{\pi}{4} + 0.5\cdot\left(1 - \frac{\pi}{4}\right) \qquad [6.27]$$

so

$$\Delta v = kb_1 w \qquad [6.28]$$

Substituting equation 6.24 into 6.28, c_{33} can be obtained:

$$c_{33} = \frac{3\pi\Delta Qhwk - 2\Delta v c_{22}\pi^2 tw^2}{6\Delta v t h^2} \qquad [6.29]$$

where v and Q can be obtained from the tested shear force–rotation relationship. If v and Q are from the shear force–rotation curve of fabric in the warp direction, c_{22} is the tensile modulus of fabric in the weft direction. Or if v and Q are from the weft direction, c_{22} must be the tensile modulus of fabric in the warp direction when stress is equal to $P/20 = 10$ gf/cm.

6.3.5 Numerical results

The above analysis has provided a picture of shear stress/strain distribution in the test specimen and a close form solution for the calculation of shear modulus of a fabric in terms of the data obtained from the KES tester. This section will deal with numerical results calculated from this solution and the accuracy and validity of the analytical solution will also be discussed.

6.3.5.1 Computation of c_{33}

c_{33} is the main focus of this study and its relation with the KES test data has been derived in equation 6.29. From equation 6.29, the computation of c_{33}

requires the value of c_{22} which is related to the tensile modulus. The tensile modulus is the value when stress = 10 gf/cm in the *y* direction, which can be obtained from the tensile curve. When the Poisson's ratio is equal to zero, c_{22} can be found from the following relationship:

$$c_{22} = \frac{E_2}{1 - \nu_{12}\nu_{21}} = E_2 = \frac{\alpha}{\beta} e^{\alpha\varepsilon} \qquad [6.30]$$

and

$$\sigma = \frac{e^{\alpha\varepsilon} - 1}{\beta} \qquad [6.31]$$

where σ is the tensile stress in gf/cm and ε the tensile strain expressed as a percentage. α and β are two constants which can be determined by the non-linear regression technique (Hu, 1994). When σ is equal to 10 gf/cm, c_{22} can be obtained from the following equation;

$$c_{22} = \frac{\alpha}{\beta}[(10 \times \beta) + 1](\text{gf/cm}) = 0.00098\frac{\alpha}{\beta}[(10 \times \beta) + 1](\text{MPa}) \qquad [6.32]$$

Or, alternatively, it can be measured on the tensile stress–strain curve when stress = 10 gf/cm. In the following section, c_{22} is calculated from equation 6.32.

6.3.5.2 Modified shear modulus from tested shear curve

In equation 6.29, *w*, *h* and *k* are known. As shown in Fig. 6.9, *h* = 20 cm = 200 mm, *w* = 5 cm = 50 mm. If the material is considered as non-linear, the modulus curve of c_{33} can be calculated from input data of *v*, *Q*, c_{22} and *t* (fabric thickness). Also, in the following computation, two fabrics are used. The values of *v* and *Q* can be obtained from the curves tested on the KES tester. The loading process is divided into 140 steps; during each step, the stress–strain relationship is assumed to be linear. When *Q* is given, ϕ can be read from the curve. From ϕ, the value of *v* can be determined from Fig. 6.15. Figure 6.16 shows the shear force–rotation curves obtained from the KES shear tester for one fabric in the warp and weft directions respectively. c_{33} can be calculated from the tested curve for warp direction or for weft direction. If the fabric is orthotropic as assumed, the modified moduli of warp and weft directions should be the same.

Figure 6.17 shows the modified shear modulus curves from the calculation. From this figure, the values from the warp and weft directions for shear modulus vary with shear strain. When the shear strain is smaller than 0.01 rad, the values of shear moduli from the warp and weft directions are very

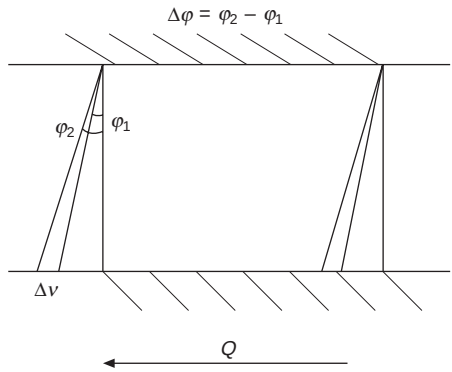

6.15 Determination of Δv.

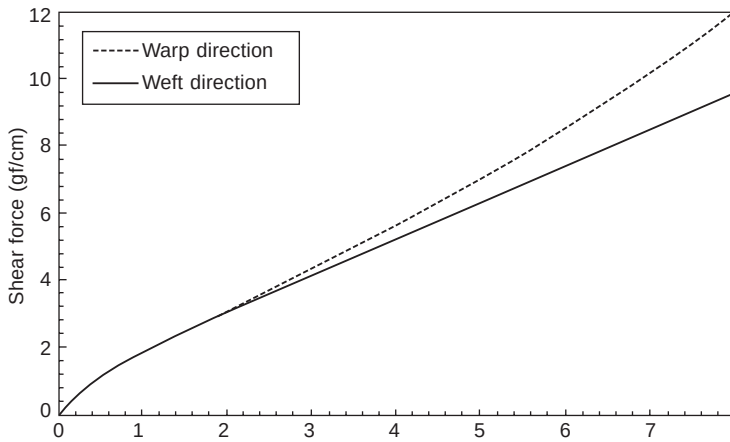

6.16 Shear force-rotation curves of KES test.

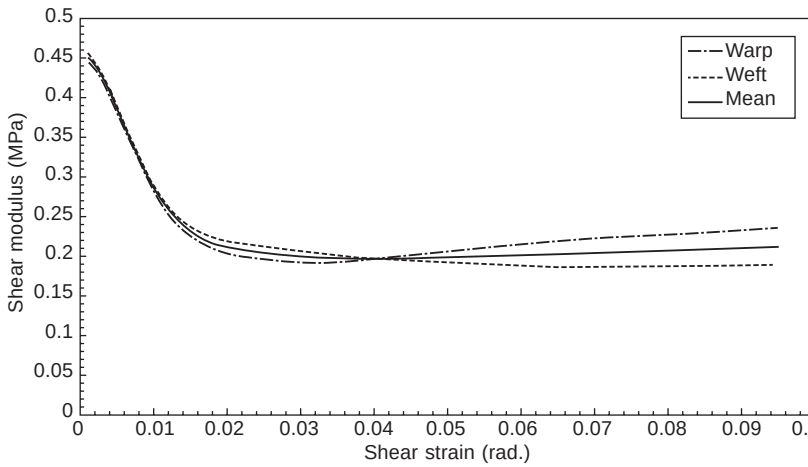

6.17 Modified shear moduli.

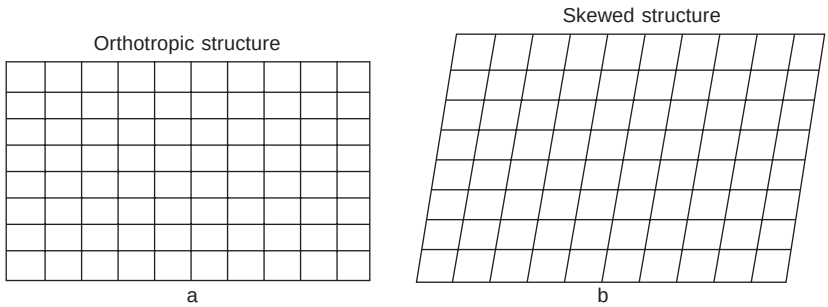

6.18 Change of orthotropic structure.

close. However, at the later stage, the difference between the warp and weft values becomes large when the strain increases. This may be due to the fact that the orthotropic assumption is inapplicable during this later stage, but valid when shear strain is very small in the initial stage.

This can be explained by Fig. 6.18. When the fabric specimen is subjected to the deformation imposed by the KES shear tester, in the initial stage, warp and weft yarns are perpendicular to each other and their rotation relative to each other is limited by internal friction between warp and weft. By contrast, in the later stage, the fabric structure is changed from state (a) to state (b), at which the warp and weft yarns are no longer perpendicular to each other. Thus the orthotropy is not held during this stage.

Therefore, the results from the present research are more accurate in the initial part of the shear deformation. In the later part, the difference between warp and weft becomes increasingly large as the shear strain increases. In view of the complexity of the later stage, it is suggested that the average c_{33} of the warp and weft values is used for representing the shear modulus of fabric sheet as shown in Fig. 6.17. Table 6.1 shows the deviations (d_1 and d_2) of warp and weft values from their averages for the fabric. The largest deviation when shear strain is 8° is around 10 % and 18 %.

6.3.5.3 Comparison of modified and tested shear moduli

From the force–rotation curve, the tangent modulus can also be derived by differentiation of force with respect to rotation angle using spline fitting. This is regarded as the tested shear modulus and represented by G, which is frequently adapted in many computations. As discussed for modified shear moduli from the warp and weft directions, tangent shear moduli directly from tested curves for the warp and weft directions are also different, thus the average values of warp and weft are used for comparison. c_{33} and G are the averages of the warp and weft directions in Fig. 6.19. The differences between the modified and tested shear moduli are listed in Table 6.2.

Table 6.1 Shear moduli of woven fabric (MPa)

γ, (rad)	c_{33}, weft	c_{33}, warp	c_{33}, average	d_1, %	d_2, %
–.0010	.4572	.4462	.4517	1.2	1.2
–.0060	.3750	.3629	.3689	1.63	1.63
–.0010	.2794	.2678	.2736	2.13	2.13
–.0160	.2335	.2214	.2274	2.68	2.68
–.0210	.2193	.2044	.2119	3.50	3.50
–.0260	.2128	.1970	.2049	3.87	3.87
–.0310	.2068	.1939	.2004	3.21	3.21
–.0360	.2026	.1942	.1984	2.11	2.11
–.0410	.1985	.1980	.1982	0.12	0.12
–.0460	.1952	.2033	.1992	2.03	2.03
–.0510	.1923	.2082	.2003	3.97	3.97
–.0560	.1904	.2130	.2017	5.61	5.61
–.0610	.1889	.2173	.2031	7.01	7.01
–.0660	.1882	.2211	.2046	8.05	8.05
–.0710	.1877	.2243	.2060	8.89	8.89
–.0760	.1882	.2272	.2077	9.41	9.41
–.0810	.1889	.2293	.2091	9.65	9.65
–.0860	.1900	.2319	.2109	9.94	9.94
–.0910	.1907	.2350	.2128	10.41	10.41
–.0960	.1913	.2387	.2150	11.02	11.02

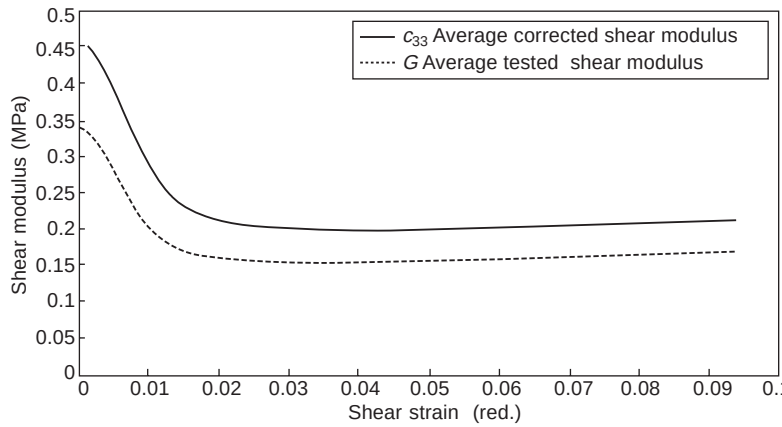

6.19 Comparison of simple and modified shear moduli.

From these two figures, the modified modulus c_{33} is consistently larger than the one derived from the tested data which corresponds to the conventional shear stiffness G. In other words, from Fig. 6.19, the shear modulus derived from the test is always smaller than the modified ones. More than 25 % and up to 32 % of error can be found in the later stage. Thus the error of the tested shear modulus is very significant.

Table 6.2 Comparison of shear moduli for woven fabric

γ (rad)	c_{33} average (MPa)	G, average (MPa)	Difference, % $(G - c_{33})/c_{33}$
.0010	.4517	.3361	–25.8
.0060	.3689	.2625	–28.8
.0110	.2736	.1932	–29.4
.0160	.2274	.1673	–26.5
.0210	.2119	.1600	–24.5
.0260	.2049	.1557	–24.0
.0310	.2004	.1536	–23.3
.0360	.1984	.1535	–22.6
.0410	.1982	.1543	–22.2
.0460	.1992	.1552	–22.1
.0510	.2003	.1562	–22.0
.0560	.2017	.1574	–22.0
.0610	.2031	.1585	–22.0
.0660	.2046	.1597	–22.0
.0710	.2060	.1609	–21.9
.0760	.2077	.1622	–21.9
.0810	.2091	.1637	–21.7
.0860	.2109	.1654	–21.6
.0910	.2128	.1674	–21.3
.0960	.2150	.1697	–21.1

6.3.5.4 *Modified shear modulus calculated from the tested parameter G*

From the KES shear test, a single value of G is given for the shear stiffness, which is the slope between shear angle of 0.5–5° as shown in Fig. 6.20. This is equivalent to considering that the shear deformation of the fabric is linear

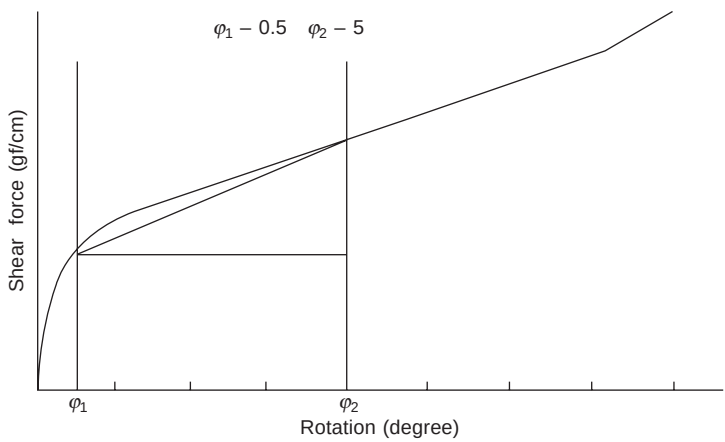

6.20 Determination of G on the KES shear tester.

Table 6.3 c_{33} calculated from G and related parameters

Sample	Direction	α	β	$0.2\times c_{22}$	G	t	c_{33}	$(0.2\times c_{22})/c_{33}$	c_{33}/G
2	weft	0.258	0.006	0.009	0.253	0.222	0.314	2.89	1.24
	warp	0.451	0.034	0.003	0.223		0.296	1.18	1.33
3	weft	0.304	0.011	0.006	0.212	0.233	0.272	2.16	1.28
	warp	0.526	0.040	0.004	0.195		0.258	1.40	1.32
4	weft	0.366	0.013	0.006	0.154	0.240	0.190	3.32	1.23
	warp	0.435	0.027	0.004	0.136		0.173	2.28	1.28
5	weft	0.271	0.008	0.007	0.220	0.230	0.277	2.55	1.26
	warp	0.474	0.035	0.004	0.200		0.265	1.35	1.32
6	weft	0.302	0.003	0.024	0.571	0.249	0.204	3.38	1.23
	warp	0.715	0.006	0.026	0.580		0.708	3.66	1.22
7	weft	0.227	0.004	0.011	0.247	0.218	0.297	3.64	1.20
	warp	0.450	0.030	0.004	0.227		0.300	1.27	1.32
9	weft	0.288	0.007	0.009	0.280	0.205	0.346	2.66	1.24
	warp	0.404	0.038	0.003	0.277		0.373	0.76	1.35
10	weft	0.290	0.006	0.009	0.210	0.179	0.242	3.92	1.15
	warp	0.556	0.033	0.004	0.185		0.235	1.87	1.37
11	weft	0.338	0.008	0.009	0.256	0.171	0.306	2.97	1.19
	warp	0.485	0.033	0.004	0.217		0.281	1.37	1.30
12	weft	0.313	0.008	0.009	0.235	0.170	0.278	3.10	1.18
	warp	0.483	0.026	0.005	0.218		0.278	1.64	1.28
13	weft	0.232	0.006	0.008	0.245	0.204	0.302	2.76	1.23
	warp	0.604	0.077	0.003	0.220		0.295	0.92	1.34
14	weft	0.296	0.006	0.011	0.208	0.240	0.247	4.32	1.19
	warp	0.509	0.047	0.003	0.192		0.255	1.22	

after the initial stage. For simplification, in many applications, the value of G is used for shear stiffness in place of c_{33}.

As mentioned earlier, this is not the correct value for pure shear deformation. It is desirable that an analytical solution can be used for calculating the shear modulus from the value of G. According to the definition of G from KES testing, equation 6.29 becomes:

$$c_{33} = 1.4\frac{f_2 - f_1}{\varphi_2 - \varphi_1} \cdot \frac{1}{t} - 0.2c_{22} = 1.4\frac{G}{t} - 0.2c_{22} \qquad [6.33]$$

Data for G from 24 fabrics were used for the calculation of c_{33}. The results are shown in Table 6.3.

It can be seen from this table that the difference between tested and modified moduli is also very large, about 25–30 %. The effect of c_{22} is not very significant. From this table and equation 6.33, the error caused by ignoring c_{22} is about 2 %. If the term containing c_{22} is ignored, the ratio of the modified and tested shear moduli is equal to 1.4 which is also applicable for continuous non-linear shear stiffness.

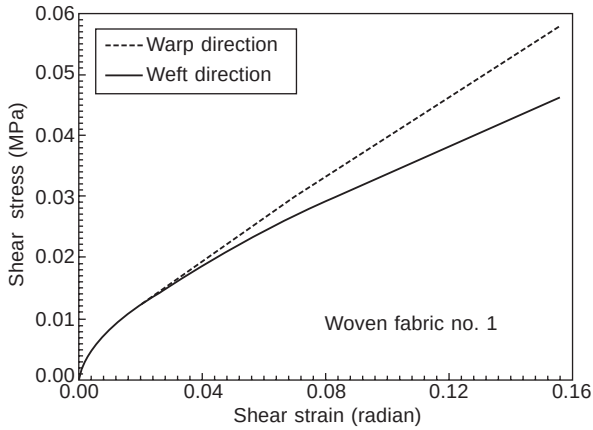

6.21 Modified shear stress–strain curve.

6.3.5.5 Stress–strain relationship

Because the shear force–rotation curve from the KES tester does not correspond to the pure shear state, it needs to be modified. The modified version can be obtained from the analytical solution for c_{33}. Within the small range of force increment, the shear stress and strain relationship is linear. Two fabrics were examined as above. The whole loading process is also divided into 140 steps, thus non-linear stress–strain curves are obtained. The shear stress–strain curves are shown in Fig. 6.21.

6.4 Shear properties of woven fabrics in various directions

6.4.1 Introduction

Shear behaviour of woven fabrics in both principal directions has received wide attention as it affects many types of fabric behaviour, but little attention is paid to the shear properties in other directions, which is no less important than that in the principal directions since garments in practical use deform in various directions. Therefore, a quantitative knowledge of the shear properties in bias directions becomes a must for garment design and new fabric development, and this is the main topic of this section.

As we all know, the shear behaviour of a woven fabric can be characterised by two shear parameters, i.e. shear rigidity (G) and shear hysteresis ($2HG$ and $2HG5$). Shear rigidity is the resistance of a fabric to shear while shear hysteresis is the energy loss within a shear deformation cycle. Existing literature has suggested a strong relationship between shear rigidity and shear hysteresis (Collier, 1991; Hu and Newton 1993; Hu, 1994; Jeong and Phillips, 1998). The results obtained from Collier, Jeong and Phillips and Hu indicated that

the correlation coefficients of shear rigidity and shear hysteresis can be as high as 0.90 or more. Based on the assumption that shear rigidity and shear hysteresis share a similar mechanism, a *G*-predicting model can be developed through the KES data collected from a wide range of woven fabrics. Furthermore, the proposed model can be further applied to predict shear hysteresis. The validity of the model for shear hysteresis, which has been visualised in the form of polar diagrams, will be confirmed, and the results also indicate a linear relationship between shear rigidity and shear hysteresis which not only holds in the principal directions, but is also present in bias directions.

6.4.2 Modelling of the anisotropy of shear properties

The classical elasticity theory is developed by Kilby (1961, 1963) based on the assumption that a fabric is an anisotropic lamina possessing a Poisson effect and with two planes of symmetry at right angles to one another. According to the elasticity theory (Hu, 1994), the behaviour of tensile and shear properties from the theoretical transformation of various compliances in the principal and bias directions can be used to yield the following equations:

$$\frac{1}{E'_X} = \frac{\cos^4\theta}{E_1} + \left(\frac{1}{G} - \frac{2\nu_{12}}{E_1}\right)\cos^2\theta\sin^2\theta + \frac{\sin^4\theta}{E_2} \qquad [6.34]$$

$$\frac{1}{E'_Y} = \frac{\sin^4\theta}{E_1} + \left(\frac{1}{G} - \frac{2\nu_{12}}{E_1}\right)\cos^2\theta\sin^2\theta + \frac{\cos^4\theta}{E_2} \qquad [6.35]$$

and

$$\frac{1}{G'_{XY}} = 4\left(\frac{1}{E_1} + \frac{1}{E_2} + \frac{2\nu_{12}}{E_1}\right)\cos^2\theta\sin^2\theta + \frac{1}{G}(\cos^2\theta - \sin^2\theta)^2 \qquad [6.36]$$

where E'_X, E'_Y and G'_{XY} denote the tensile modulus in the X' and Y' axes and shear rigidity between both principal directions respectively with an angle θ.

With equation 6.32, the shear rigidity in the X' and Y' axes can be obtained directly from experimental tensile modulus, while ν_{12} cannot. The theoretical treatment suggests that measurements of modulus in two directions are insufficient to define a fabric's shear rigidity, since variations with direction are still possible for fabrics with similar E_1 and E_2. An investigation of the third direction is therefore necessary, and the most convenient direction is the 45°. Thus, the sum $(1/E_1 + 1/E_2 + 2\nu_{12}/E_1)$ may be deduced from measurements in three directions by considering specimens cut along the warp, weft and 45° directions. Therefore, when considering $\theta = 45°$ values, equation 6.32 gives

$$\frac{1}{G_{45}} = 4\left(\frac{1}{E_1} + \frac{1}{E_2} + \frac{2\nu_{12}}{E_1}\right)\left(\frac{1}{\sqrt{2}}\right)^2\left(\frac{1}{\sqrt{2}}\right)^2 \quad [6.37]$$

and

$$\frac{2\nu_{12}}{E_1} = \frac{1}{G_{45}} - \frac{1}{E_1} - \frac{1}{E_2} \quad [6.38]$$

Substituting equation 6.37 into equation 6.32, we get

$$\frac{1}{G_\theta} = \left(\frac{1}{G_{45}}\right)\cos^2\theta\sin^2\theta + \frac{1}{G}(\cos^2\theta - \sin^2\theta)^2 \quad [6.39]$$

Thus fabric shear rigidity in various directions can be predicted from equation 6.39 when its values in the warp and ± 45° directions are measured. As shear rigidity provides a measure of the resistance to the rotational movements between the warp and weft yarns at the intersecting points when the fabric is subjected to a small shear deformation, its relationship between both principal directions should be determined. That is, a strong linear relationship is obtained in the two principal directions by Mahar *et al*. (1989, 1990) and it is elucidated that the measurement on fabric shear properties can be simplified and is necessary in only one principal direction. It is further proved from equation 6.39 that the shear rigidity in either the warp or weft direction with ± 45° directions gives a very satisfactory result in various directions. However, if the differences in the values of shear rigidity between the warp and weft directions are large, the average value will be taken in both principal directions in the calculation of shear rigidity in various directions given in equation 6.39.

Shear hysteresis of the fabric can be defined as the energy loss within the shear cycle when the fabric is deformed and allowed to recover to its original position. Since strong linear relationship between shear rigidity (G) and shear hysteresis ($2HG$ and $2HG5$) has been proved by several researchers (Collier, 1991; Hu, 1994; Jeong and Phillips, 1998), the proposed G-predicting model in different directions can be applied to shear hysteresis ($2HG$ and $2HG5$) of different fabrics.

6.4.3 Polar diagrams of the shear model

6.4.3.1 General features

As shown by Figs 6.22 and 6.23, the shear parameters, i.e. shear rigidity G and shear hystereses, $2HG$ and $2HG5$, exhibit great similarities. First, the shapes of their polar diagrams are all symmetrical to the warp and weft directions. Second, the values of these parameters change with the angle with their maxima exactly at ± 45° to the warp or weft direction. Therefore,

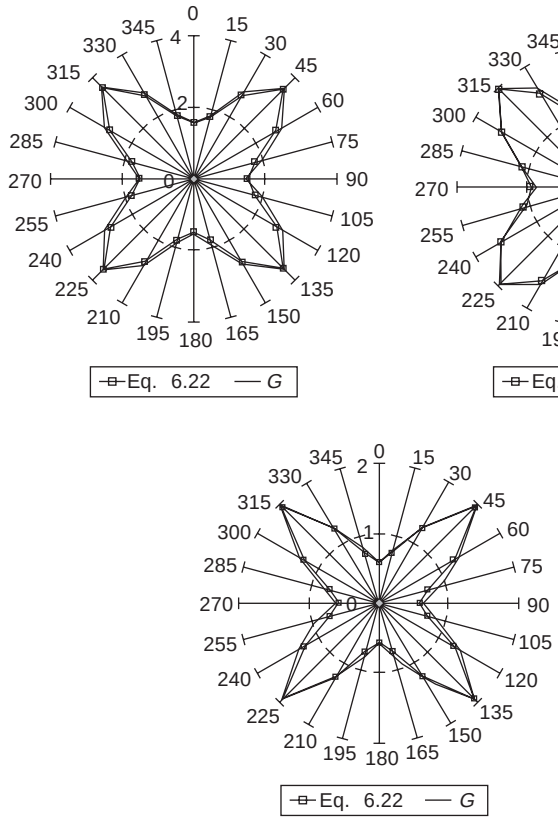

6.22 Typical polar diagram of shear rigidity (*G*).

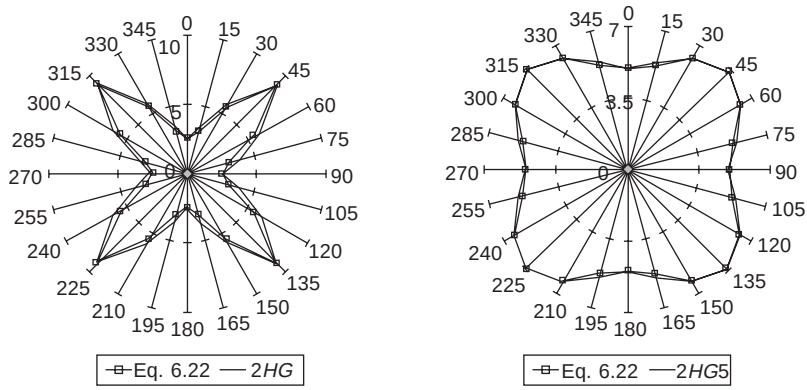

6.23 Typical polar diagram of shear hysteresis (2*HG*, 2*HG*5).

the shape of these polar diagrams is mainly governed by their values at ± 45°. Presumably, the anisotropy of the shear rigidity should be due to some inherent difference in their physical behaviour, the types of finishes undergone and the stiffness of the constituent yarns or fibres, the contact area at the intersecting points of two sets of yarns, the fibre packing density in the yarns, and so on. As a result, any combination of these factors can confer different shear characteristics in woven fabrics even when produced in the same material.

From fabric geometry, there is a normal pressure acting at each intersecting point of two sets of yarns in the unset fabric. As the shear force is applied to the fabric and usually has a larger magnitude than the frictional restraint at the intersecting point of yarns, the fabric will deform with hysteresis effect. In this case, the fabrics woven with natural fibres will have larger value of shear hysteresis than those with synthetic fibres due to the relatively low contact area of synthetic fibres at each yarn intersecting point.

The values of shear properties will be decreased after the finishing process. It is a fact that the residual bending stress existing in the yarns is released with the drop of the normal reaction acting on the crossing over regions. Thus commercially available woven fabrics usually have lower values of shear properties than laboratory-produced woven fabrics.

As the shear deformation depends upon the frictional and elastic forces within a fabric, elastic force will be built up rapidly if tightly woven fabric is sheared where limited sliding of yarns over each other is allowed in their crossing over points. On the contrary, the frictional forces will be very low if the fabric is loosely constructed and produced in weaves such as twill and satin.

6.4.3.2 Effect of weave density on fabric shear

In this section, our discussion is based on the analysis of plain and twill fabrics. Because the warp densities of these fabrics are kept constant, any changes in the trends of polar diagrams of shear properties can be considered to be due to the different weft densities of these fabrics. The polar diagrams of shear rigidity and shear hysteresis with different weft densities are plotted in Fig. 6.24.

The highest shear rigidity and shear hysteresis are observed from the plain fabrics while the lowest is found from the 3/3 twill fabrics shown in Fig. 6.23. For different weft densities, the results obtained from Fig. 6.24 show that the values of shear rigidity and shear hysteresis increase with the increase in the weft density of woven fabrics. From all experimental results, the shape of the polar diagrams moves inward to outward when the fabric weave density increases. This is because a loose structure has lower inter-yarn friction and allows the relative movement of warp and weft yarns. As

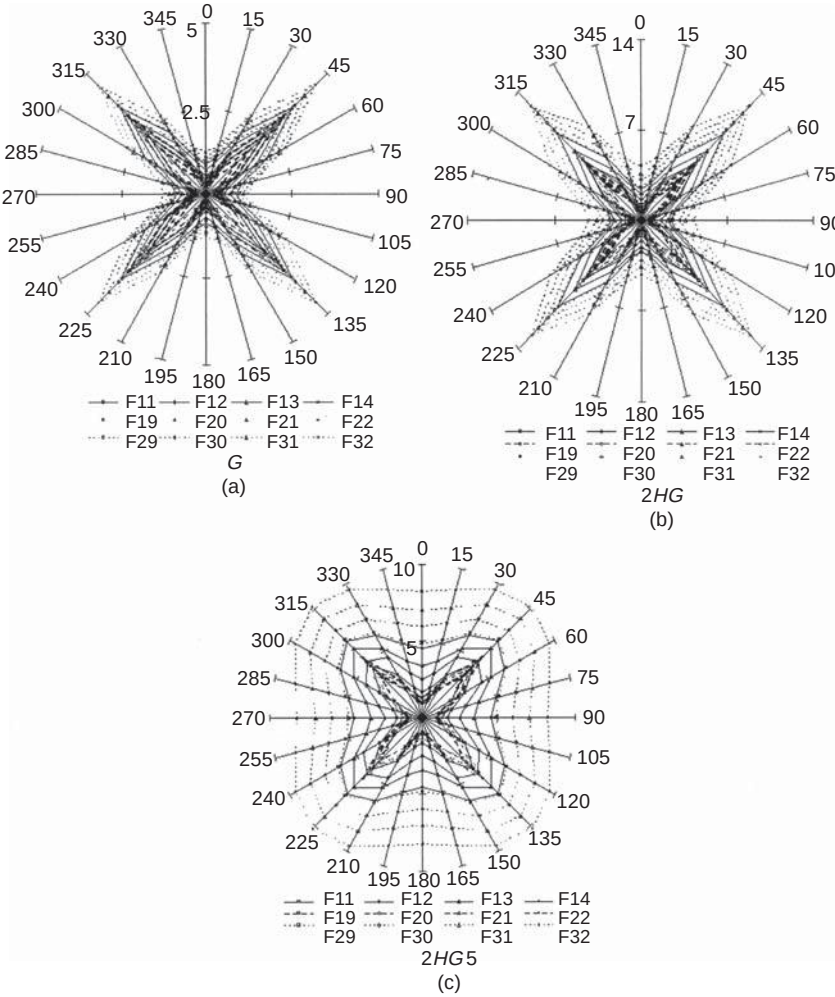

6.24 Effect of weft density on the polar diagrams of shear parameters: (a) *G;* (b) 2*HG;* (c) 2*HG*5.

a result, loose fabrics have the lowest shear rigidity and shear hysteresis. On the other hand, a tight structure avoids yarn movement, thus increasing the shear hysteresis of the fabrics. Therefore, a larger value of shear rigidity and shear hysteresis leads to an increase in the size of the polar diagram.

6.4.4 Relationship between shear rigidity and hysteresis in various directions

Existing literature shows a strong relationship between shear rigidity and shear hysteresis (Collier, 1991; Hu, 1994; Jeong and Phillips, 1998). The

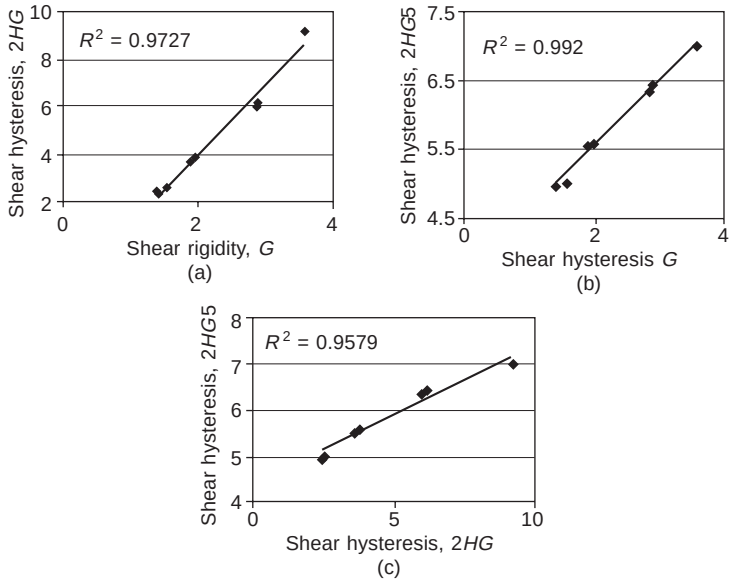

6.25 Relationship between shear rigidity and hysteresis in various directions: (a) 2*HG* and *G;* (b) 2*HG*5 and *G;* and (c) 2*HG*5 and 2*HG.*

relationships between shear rigidity (*G*) and shear hysteresis (2*HG* and 2*HG*5) of a fabric sample in various directions are illustrated in Fig. 6.25 parts (a)–(c) respectively. It can be seen that a strong linear relationship exists between shear properties in different directions. The coefficient of determination R^2 for 2*HG* and *G* in various directions is 0.9727, for 2*HG*5 and *G* in various directions is 0.9920 and for 2*HG*5 and 2*HG* in various directions is 0.9579. These strong linear relationships between shear rigidity and shear hysteresis at two angles, $R^2 > 0.90$, are also held in many other types of woven fabrics.

From these facts, it can be assumed that a similar mechanism operates for shear rigidity and hysteresis between both principal directions and bias directions. As shear rigidity of a fabric is mainly caused by the frictional forces existing in the yarns, shear hysteresis is also governed by its corresponding frictional force and the occurrence of the frictional force is continuous in the whole shear cycle. Higher values of shear rigidity appear in the bias directions and larger magnitudes of shear hysteresis can be found in these directions too.

6.5 Summary

Whenever bending occurs in more than one direction, so that the fabric is subject to double curvature, shear deformations of the fabric are involved. It

is thus not strange to find a strong relationship between the shear property and the bending property. Shear deformation is very common during the wearing process since the fabric needs to be stretched or sheared to a greater or lesser degree as the body moves. This chapter provides a comprehensive knowledge of the shear properties of woven fabrics and the conclusions reached include:

(1) The statement that bending and shear have identical nature is doubtful. The hardening of warp yarns has little effect on shear properties, but cover factor has a definite influence. Generally, large cover factor will produce large shear stiffness and shear hysteresis before the jammed condition is reached. After that, this effect is not apparent. The relation between bending and shear is not as strong as some literature has stated and, for some fabric types, like shengosen fabrics, they are totally different. This is because the two deformation modes operate in different ways although they both involve friction and yarn bending.

(2) The shear modulus and curves obtained on the KES shear tester are significantly different from those under the pure shear state, but they are still a good reflection of the shear properties of woven fabrics. Finite-element analysis can be successfully used to analyse the distribution of shear stresses and strains determined on the KES tester. The exact shear stress–strain relationship and actual shear modulus need modification for complex fabric deformation.

(3) A model derived from Kilby's work can be successfully used to predict the shear rigidity in all directions and extended to predict the shear hysteresis due to a strong linear relationship between them, which exists not only in the warp and weft directions but also in the bias directions. The shape of polar diagram of fabric shear properties is symmetrical to the warp and weft directions and has a crest given the maximum values in ± 45° directions. Moreover, the polar diagrams of shear rigidity and shear hysteresis will move outwards with the increase in weave density.

6.6 References

Behre B (1961), Mechanical properties of textile fabrics part I: shearing, *Text Res J*, **31**(2), 87–99.

Chapman B M (1980), Viscoelastic, frictional and structural effects in Fabric Wrinkling, in *Mechanics of Flexible Fibre Assemblies* (NATO Advanced Study Institute Series No. 38), Hearle J W S, Thwaites J J and Amirbayat J (eds), The Netherlands, Alpen ann den Rijn, Sijhoff and Noordhoff.

Collier B J (1991), Measurement of fabric drape and its relation to fabric mechanical properties and subjective evaluation, *Clothing & Text. Res J*, **10**(1), 46–52.

Collier J R, Collier B J, Toole G O and Sargrand S M (1991), Drape prediction by means of finite element analysis, *J Text Inst*, **82**(1), 96–107.

Cusick G E (1961), The resistance of fabrics to shearing forces, *J Text Inst*, **52**(9), T395–406.

Dawes V and Owen J D (1971), The assessment of fabric handle, *J Text Inst*, **62**, 233.

Dreby E C (1941), The planoflex: a simple device for evaluating the pliability of fabrics, *American Dyestuff Reporter*, **30**, 651–666.

Gan L, Steven G P and Ly N (1991), A finite element analysis of the draping of fabric *Proc 6th, Int Con in Australia on Finite Element Methods*, University of Sydney, Australia, July 8–10, 7.

Go Y, Shinohara A and Matsuhashi F (1957), Viscoelastic studies of textile fabrics part III: on the shearing buckling of textile fabrics, *Sen-i Gakkaishi*, **13**, 460–65.

Grosberg P and Park B J (1966), The mechanical properties of woven fabrics part V: the initial modulus and the frictional restraint in shearing of plain woven fabrics, *Text Res J*, **36**, 420–431.

Hu J L (1994), *Structure and Low Stress Mechanics of Woven Fabrics* (PhD thesis, University of Manchester Institute of Science and Technology).

Hu J L and Newton A (1993), Modelling of tensile stress–strain curves of woven fabrics, *J China Text Univ*, **4**, 49–61.

Jeong Y J and Phillips D G (1998), A study of fabric-drape behaviour with image analysis part II: effect of fabric structure and mechanical properties on fabric drape, *J Text Inst*, **89**(1), 70–79.

Kang T J, Lee J, Yu W R and Oh K H (1994), Prediction of woven fabric deformation using finite element method, *Proceedings of the International Symposium on Fibre Science and Technology*, **8**, 480.

Kawabata (1972), *Kawabata's Evaluation System for Fabric (KES-FB) Manual*, Kyoto, Kato Tech Co Ltd.

Kawabata S (1980, July), *Standardisation and Analysis of Hand Evaluation, 2nd ed*, Osaka, Textile Machinery Society of Japan.

Kawabata S, Niwa M, Ito K and Nitta M (1972), Application of objective measurements to clothing manufacture, *Int J Clothing Sci & Tech*, **2**(3/4), 8–31.

Kilby W F (1961), Shear properties in relation to fabric hand, *Text Res J*, **31**, 72–73.

Kilby W F (1963), Planar stress–strain relationships in woven fabrics, *J Text Inst*, **54**, T9–27.

Lindberg J, Behre B and Dahlberg B (1961), Mechanical properties of textile fabrics part III: shearing and buckling of various commercial fabrics, *Text Res J*, **31**(2), 99–122.

Lloyd D W, Shanahan W J and Konopasek M (1978), The folding of heavy fabric sheets, *Int J Mech Sci*, **20**, 521–527.

Lo W M (2001), *A Study of Fabric Anisotropy* (PhD Thesis, The Hong Kong Polytechnic University).

Lo W M and Hu J L (2002), Shear properties of woven fabrics in various directions, *Text Res J*, **72**(5), 383–390.

Lucas (1994), *FEA User's Manual and Theory Manual*, UK, Finite Element Analysis Ltd, Surrey.

Mahar T J, Dhingra R C and Postle R (1989), Fabric mechanical and physical properties relevant to clothing manufacture part I: fabric overfeed, formability, shear and hygral expansion during tailoring, *Int J Clothing Sci & Tech*, **1**(1), 12–20.

Mahar T J, Dhingra R C and Postle, R (1990), Measuring and interpreting low stress fabric mechanical and surface properties, *Textile Research Journal*, **60**, 7–17.

Mark C and Taylor H M (1956), Fitting of woven cloth to surfaces, *J Text Inst*, **47**, T477.

Morner B and Eeg-Olofsson T (1957), Measurement of the shearing properties of fabrics, *Text Res J*, **27**, 611–614.

Okabe H and Akami H (1984), The estimation of the three dimensional shapes of garments, *Report to the Polymer Materials Research Institute*, Japan, No, 142.

Oloffson B (1967), Study of inelastic deformations of textile fabrics, *J Text Inst*, **58**, 211.

Postle R, Carnaby G A and de Jong S (1976), Woven fabric shear and bending, *The Mechanics of Wool Structures*, Chichester, Ellis Horwood, 340–366.

Skelton J S (1976), Fundamentals of fabric shear, *Text Res J*, **46**, 862–869.

Skelton J S (1980), Shear of woven fabrics, in *Mechanics of Flexible Fibre Assemblies* (*NATO Advanced Study Institute Series; E Applied Sciences No. 38*), Hearle J W S, Thwaites J Je and Amirbayat J (eds), The Netherlands, Alpen ann den Rijn, Sijthoff and Noordhoff, 211–227.

Skelton J S and Schoppee M M (1976), Frictional damping in multicomponent assemblies, *Text Res J*, **46**, 661.